Energy parameters of a hybrid counter-rotor hydraulic unit operating on the basis of solar and hydraulic energy

Oybek Bozarov[1*], *Rayimjon* Aliyev[2], *Dilshod* Kodirov[3], *Hamidillo* Usarov[4]

[1]Tashkent State Technical University, Tashkent, Uzbekistan
[2]Andijan State University, Andijan, Uzbekistan
[3]Department of Power Supply and Renewable Energy Sources, National Research University TIIAME, Tashkent, Uzbekistan
[4]Andijan Institute of Agriculture and Agrotechnologies, Andijan, Uzbekistan

Abstract. This article analyzes the prospects for using a combined hybrid solar photovoltaic and hydroelectric device and presents their characteristics and energy parameters. In particular, since the hydroelectric device consists of a counter-rotor hydraulic unit, the functional relationship between the dynamic parameters of the reactive and active impellers and the efficiency of the hydraulic unit was investigated. Based on the obtained graphs and analytical expressions, the relationship between the energy parameters of the jet nozzle hydraulic turbine and the design parameters of the hydraulic unit was analyzed.

1. Introduction

It is no secret that the uneven distribution and limitation of underground fuel resources on our planet harms economic dependence on fuels among countries. The ever-increasing demand for heat and electricity on a global scale is causing the price of underground fuels to increase. This situation creates a demand for rational use of renewable energy sources in all fields.

The development of semiconductor photovoltaics is characterized by new areas of applied scientific research. Semiconductor photoelectric converters (FP) are divided into three generations: FP of the first generation; 2nd generation FP and 3rd generation FP. Active research is being conducted on the development of second and third generation AF. The emergence and intensive development of digital modeling methods made it possible to raise the quality of research to a significantly higher level. The possibility of a comprehensive implementation of the theory of classical and quantum solid state physics, the formation of information bases of a multitude of experimental data made it possible to carry out scientific research with better quality, intensity and results.

In this regard, the following most important directions in fundamental scientific and applied terms can be noted. First, it deserves special attention that multilaterally illuminated elements can be created on the basis of the first-generation FP [1]. Theoretical and experimental studies carried out in this direction testified to the good prospects for the creation of matrix FPs with vertical p-n junctions. Such PCs are dominated by indisputable advantages in the tasks of generating high output voltages and converting concentrated solar radiation. In addition, the implementation of such FPs in a multilaterally sensitive design makes it possible to reduce the consumption of semiconductor silicon by up to three to four times.

Secondly, of great interest is scientific and applied research related to the operation of the FP in a dry, hot, continental and dusty climate, for example, in the republics of Central Asia. Therefore, the tasks of creating solar photovoltaic devices adapted to continental climate change remain relevant. In this regard, it is promising to develop and implement solar photovoltaic power plants in 3D format, in which the use of flat panels is excluded for the first time [2]. It should be noted that such power plants are competitive for converting concentrated solar radiation.

The natural instability of the primary potentials of renewable sources remains an unresolved problem throughout the world. Therefore, in order to obtain continuous energy from renewable sources, active applied research is being carried out to create hybrid power plants: "Solar-wind"[3], "Solar-photovoltaic", "Solar-photovoltaic-thermal", "Solar-hydraulic"[4], "Wind-hydraulic" and "Solar-wind-hydraulic".

Based on the results of this research, the cost of solar devices developed will decrease, and their economic efficiency will increase. However, the accumulation of a large amount of solar radiation in a small volume causes the

*Corresponding author: obozarov7@inbox.ru

temperature of the device to rise rapidly. It is known that such a situation is also observed in existing solar panels. Their temperature during operation rises to 80-850C. As a result, its efficiency decreases sharply. Therefore, it is advisable to use an energy-efficient method of cooling the solar panels.

To eliminate the heating of solar elements, various methods are offered on a global scale today. In particular, the automated system of water cooling in Uzbekistan [5], the scientist of the University of Saudi Arabia, Imam Abdurakhman bin Faisal, studied active and passive cooling systems [6]. They evaluated the effectiveness of different methods of cooling photovoltaic devices. They found that cooling the back of the solar cell through tubes filled with ethylene glycol or pure water was most effective. Therefore, in the cooling system of solar panels, it is envisaged to use a radiator with water flowing through it, placed behind the panel. Water circulation in these radiators is carried out using a pump system. In this case, the signal data received from the thermosensor on the solar panel is processed in the main control center, which also controls the pump operation mode. In the process of cooling the solar panels, the pumps receive electricity from the hydroelectric plant through a central control system.

Most of the places where micro hydropower plants can be built are in uninhabited areas or far from the public grid. In order to supply the electricity produced by the micro hydroelectric power stations built in such places to the general network, additional electrical engineering devices are required. These devices lead to an increase in the cost of electricity. Therefore, it will not be profitable to produce electricity in these places and sell it through the public grid. But using this obtained electricity, it is possible to produce environmentally friendly hydrogen fuel in these areas. This continuously generated electricity is stored as hydrogen fuel.

Based on the above considerations, the authors considered a hybrid system consisting of solar and hydroelectric power plants suitable for local conditions.

The main task in the development of a hybrid system is the selection of devices for controlling the power ratio of solar and hydroelectric power plants and their operating modes. Depending on the monthly electricity production from a certain source under certain conditions, it is possible to determine which source is used as the main one and which one as an auxiliary one. When several sources work with a single control and energy conversion unit, the relative cost of the entire power plant can be reduced, and as a result, the unit cost of electricity per kWh decreases. Therefore, it is necessary to analyze the energy parameters of the devices participating in the system and ensure the mutual compatibility of the parameters of the devices.

2. Methodology

2.1 Organizational parts of the hybrid electric system

Below is a general block diagram of the proposed hybrid power plant (Fig.1).

Combined hybrid system components consist of solar panels, solar panel cooling system, counter-rotor hydro unit, main control center, control shaft, electric storage block and consumer.

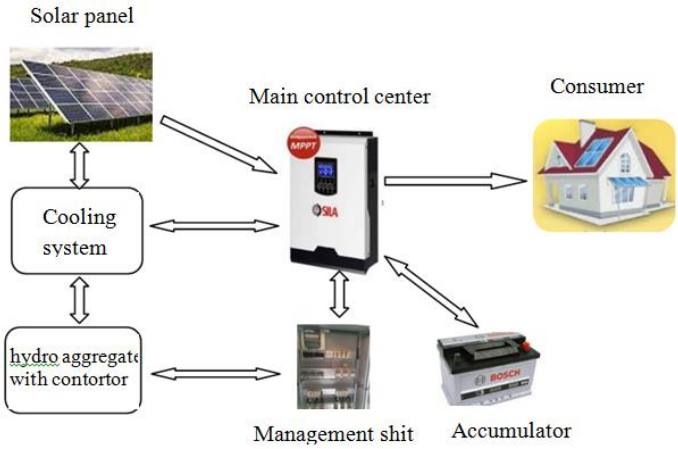

Fig.1. General block diagram of a hybrid power plant based on a solar power plant and a counter-rotor hydroelectric unit

The flow of water entering from the supply pipe of the hydraulic aggregate 1 is directed through the cylinder of the internal diverting device 2 from the diverting blades to the inlet of the nozzle 3. The water flow enters the nozzle through the cylinder of the working wheel, and after impacting with the inner walls of the nozzle 4, exits the nozzle 5 in the confusor-like exit nozzle. A bunch of water coming out of the nozzle at a speed ϑ_n hits the blades 7 located vertically in rings 6. The speed of the water shaft when the active wheel hits the blades is equal to the difference

between the relative speed of the water at the working wheel and the linear speed ϑ_l of the working wheel at a distance R_c. The change in time of the moment of the amount of movement of the water coming out of the nozzle to the impeller creates a turning moment (Fig. 2).

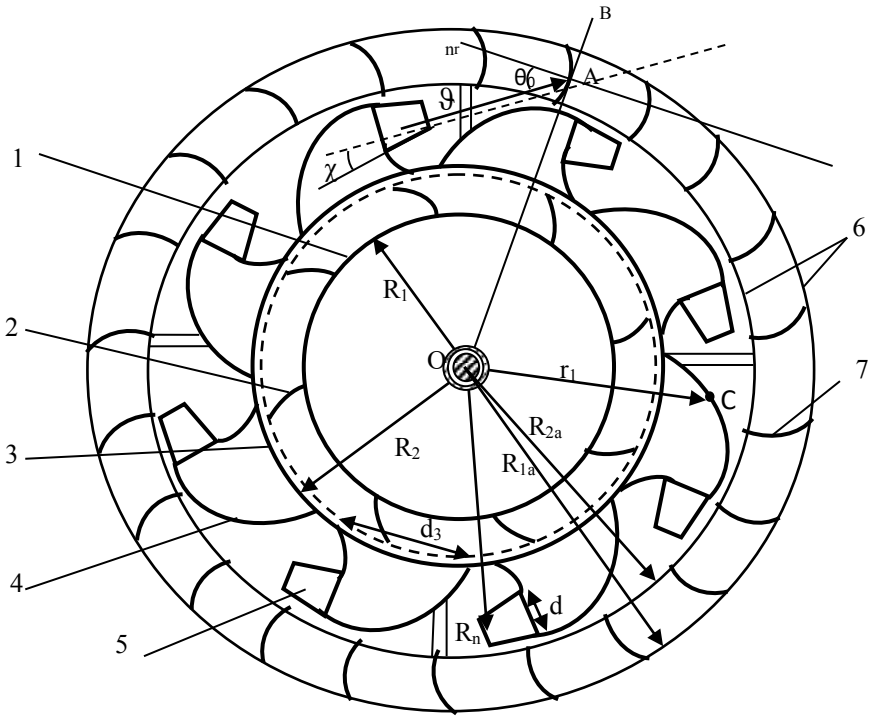

Fig. 2. Horizontal cross-section (top view) general diagram of counter-rotor hydrounit

2.2 Energy parameters of counter-rotor hydroaggregate jet hydroturbine

In the work under consideration, a counter-rotor hydro aggregate is used as the main energy generating device. The counter-rotor hydrounit consists of a nozzle jet hydro turbine and an active water wheel attached to inner and outer shafts located in a common center. The energy parameters of the counter-rotor hydrounit mainly depend on the geometric and dynamic parameters of the organizational parts of the jet hydroturbine.

The general scheme of the horizontal section of the counter-rotor hydroaggregate from above is presented in Fig. 2.

The speed of movement of water in the pipe ϑ_a is the geometric sum of ϑ_l linear speed of rotation of the impeller and the relative velocities of the water ϑ_r directed along the radius from the center of the circle.

The resulting reactive force acting on the point representing the pressure center S in Fig. 1 is equal to the vector difference of the impulses of the water jet K_3 entering the nozzle and K_c leaving it:

$$F=K_c - K_3.$$

The momentum of the water flow at the inlet and outlet of the nozzle:

$$K_n = \rho S_n \vartheta^2; \qquad K_3 = \rho S_n \vartheta_3^2; \tag{1}$$

where ρ is the water density, ϑ is the average relative velocity of the water exiting the nozzle.

From the general theorem on the change of the kinetic moment of a rigid body, the following result representing the moment of the turning force was obtained [3]:

$$M_z = -N\rho\pi R_c^3 \vartheta_c(\vartheta_c - \omega_z R_c) = -N\rho\pi R_c^3 \vartheta_c^2(1-\cos\beta). \tag{2}$$

Here, R_c is the distance from the axis of rotation to the center of the water outlet nozzle, r_c is the radius of the water outlet channel of the nozzle, N is the number of nozzles, ϑ_3, ϑ_c are the velocities of water entering and exiting the nozzle, respectively.

2.3. Water flow exit parameters from jet hydro turbine nozzle

The increase in absolute velocity ϑ_n of the jet of water coming out of the nozzle of the jet hydro turbine causes the jet force generated in the nozzle to increase, thus the shock force to the active wheel. The increase in the speed of the

water jet, the amount of the cross-sectional surface of the jet when it hits the active beam depends on the geometric shape of the nozzle, in particular, the confluence angle χ of the water outlet nozzle located at a distance of R_c radius.

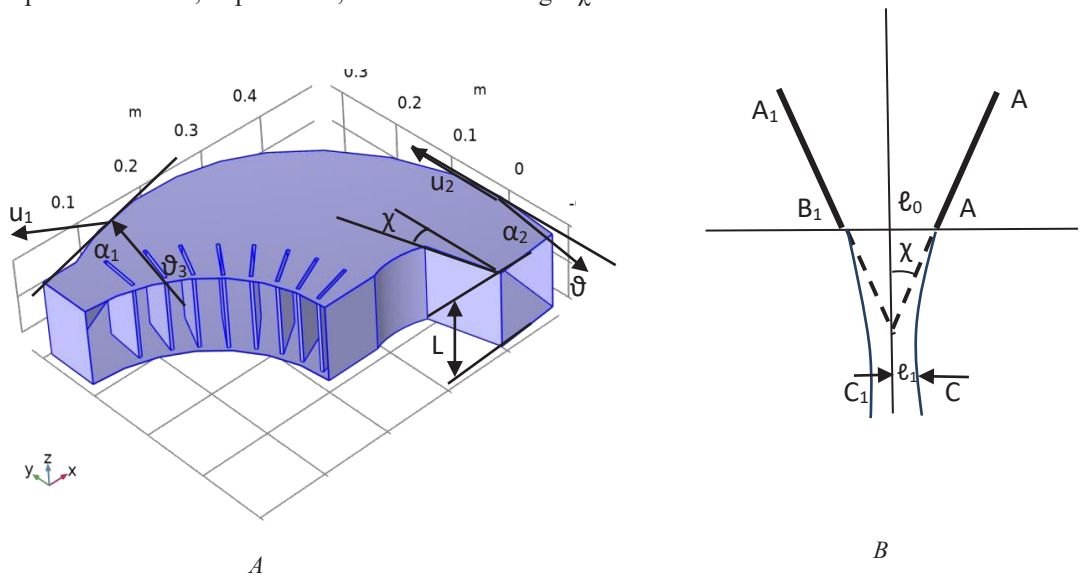

A *B*

Fig. 3. Jet Impeller Nozzle: A) Construction of a triangle of velocities for the flow of water in the nozzle; B) change in the speed and width of the water flow coming out of the nozzle

Therefore, consider the change in speed and width of the water jet as it flows out of the nozzle. As shown in Figure 4, we choose the x and y axes in the complex z plane. Let us determine the angle at which the walls of the nozzle baffle are inclined to the negative axis Ox, through -χ, the height of the nozzle L, the width of the outlet hole BB_1 through $2\ell_0$ and, we determine the water flow rate through q.

If we denote the width of the jet at infinity by $2\ell_1$, and the speed of the jet at infinity by ϑ, we have the exact relationship (Fig. 3, B).

$$q = 2L\ell_1\vartheta. \tag{3}$$

To fully determine ℓ_1 and ϑ we will need to find one more relationship between the unknown quantities ℓ_1 and ϑ and the given ℓ_0, α, q. This problem is solved using the Zhukovsky-Mitchell method.

According to the idea of Planck N.E. Zhukovsky, as well as Mitchell, proposed a modification of the Kirchhoff method, which consists in replacing the function $\frac{1}{\upsilon} = \frac{dz}{d\omega}$ through the function $Z = \ln\left(\frac{\overline{\upsilon_\infty}}{\upsilon}\right)$ and then searching for a conformal mapping of the cut plane ω onto that part of the Z plane that corresponds to the flow region in the z plane.

For the problem of the outflow of a liquid from a vessel bounded by two infinite symmetrical walls, the equations of the jet are obtained and the width of the jet at infinity is determined [7]:

general formula

$$\vartheta\frac{dz}{d\omega} = e^z; \tag{4}$$

leads in this case to the relation

$$dz = \frac{1}{\vartheta}e^{i\theta}d\varphi; \tag{5}$$

because

$$dz = dx + idy,\ d\varphi = \frac{q}{2L\chi}ctg\frac{\pi\theta}{2\varphi}d\theta; \tag{6}$$

then we get:

$$dx = \frac{1}{\vartheta}\cos\theta d\varphi = -\frac{q}{2\chi L\vartheta}\cos\theta ctg\frac{\pi\theta}{2\chi}d\theta;\ dy = \frac{1}{\vartheta}\sin\theta d\varphi = -\frac{q}{2\chi L\vartheta}\sin\theta ctg\frac{\pi\theta}{2\chi}d\theta. \tag{7}$$

Integrating (7) these relations and taking (3-5) into account that at point B with θ= -χ we have x=0, y=ℓ_0, we obtain the final equations for the aircraft jet:

$$x = -\frac{q}{2\chi L\vartheta}\int_{-\chi}^{0}\cos\theta\operatorname{ctg}\frac{\pi\theta}{2\chi}d\theta; \qquad y = \ell_0 - \frac{q}{2\chi L\vartheta}\int_{-\chi}^{0}\cos\theta\operatorname{ctg}\frac{\pi\theta}{2\chi}d\theta; \tag{8}$$

The jet width at infinity is $2\ell_1$, then $y\to\ell_1$ as $\theta\to 0$, and we get the relation

$$\ell_1 = \ell_0 - \frac{q}{2\chi L\vartheta}\int_{-\chi}^{0}\sin\theta\operatorname{ctg}\frac{\pi\theta}{2\chi}d\theta. \tag{9}$$

Combining it with equality (1) we find the value of ϑ for our case:

$$\vartheta = \frac{q}{2L\ell_0}\left[1+\frac{1}{\chi}\int_{0}^{\chi}\sin\theta\operatorname{ctg}\frac{\pi\theta}{2\chi}d\theta\right]; \tag{10}$$

and for jet compression the value:

$$\frac{\ell_1}{\ell_0} = \frac{q}{2L\ell_0\vartheta} = \frac{1}{1+\frac{1}{\chi}\int_{0}^{\chi}\sin\theta\operatorname{ctg}\frac{\pi\theta}{2\chi}d\theta}. \tag{11}$$

2.4 Energy parameters of the water wheel from the counter-rotor hydraulic unit

The results obtained above represent the relative velocity ϑof the water flow with respect to the nozzle. The speed of the water jet hitting the vanes of the active wheel is equal to the velocity $\mathbf{v}_j$of the water stream coming out of the j-nozzle in the reference system connected to the ground, that is, it is equal to the vector sum of the linear velocity u_t around the circle of the point of the jet impeller at a distance R_n with the relative speed ϑ_2:

$$\mathbf{v}_j=\boldsymbol{\vartheta}+\mathbf{u}_t. \tag{12}$$

Since the water outlet direction of the nozzle is perpendicular to the radial direction, the angle between the vectors is 180°, in this case the vector sum (12) is equal to the following algebraic difference:

$$v_j=\vartheta- u_t. \tag{13}$$

The result of $u_t=0.62\vartheta$ was obtained by constructing a triangle of velocities at the angle $\alpha_1=35°$ of the water flow entering the nozzle and $\alpha_2=10°$ with respect to the nozzle exit wall and solving it with respect to u_t(Fig. 3, A). In that case:

$$v_j=\vartheta-0.62\vartheta=0{,}38\vartheta;$$

$$v_j=\frac{0{,}38q}{2L\ell_0}\left[1+\frac{1}{\chi}\int_{0}^{\chi}\sin\theta\operatorname{ctg}\frac{\pi\theta}{2\chi}d\theta\right]. \tag{14}$$

The active water wheel is hit by a shaft of water with a speed v_j and rotates with an angular speed ω_w. It is known from the literature that the linear speed of rotation of water wheels with optimal parameters is equal to half of the speed of the water shaft acting on it [8]. Then the radius of the active working wheel:

$$R_w = 0{,}5\frac{v_j}{\omega_w};$$

$$R_w = \sqrt{0{,}5\cdot(R_{1a}^2+R_{2a}^2)}. \tag{15}$$

Amount of water acting on active wheel:

$$Q = Nq = NS_j\vartheta. \tag{16}$$

The total power of the water hitting the water wheel is equal to:

$$P_t = \frac{N\rho S_j\vartheta v_j^2}{2}. \tag{17}$$

The jet of water coming out of the jet turbine nozzle hits the blades of the active wheel at an angle θ_0 relative to the perpendicular transferred to the radial direction (Fig. 2). The n_r direction component of the force acting on the blade during impact creates a turning moment of the water wheel. The force impulse acting on the water wheel from a single nozzle:

$$F_j = \rho L\ell_1\vartheta v_j\cos\theta_0 \tag{18}$$

Full power torque:

$$M_{at} = \sum_j F_j R_w ;$$

$$M_{aj} = F_j R_w . \quad (19)$$

Useful power of active water wheel:

$$P_{efa} = M_{at} \omega_w . \quad (20)$$

Impeller Efficiency:

$$\eta_w = \frac{P_{efa}}{P_t} \cdot 100\% . \quad (21)$$

4. Results and Discussions

4.1 Results from theoretical calculation of a jet turbine's energy parameter

Table 1 shows the dependence of hydroturbine water consumption on its capacity with a step of 0.5m for 5 different sizes of hydroturbines with a water level of 1.5m to 6m.

Table 2 shows the dependence of the size of the hydro turbine on its power with a step of 0.5 m in the range of 1.5m to 6 m for 5 different constant water consumptions [9,10]

Table 1. The dependence of water consumption on its power when the size of the hydroturbine remains unchanged

№	*H, m*	*d_1=0,3 m*		*d_1=0,35 m*		*d_1=0,4 m*		*d_1=0,45 m*		*d_1=0,5 m*	
		Q (m^3/s)	*P (W)*	*Q (m^3/s)*	*P W*	*Q, m^3/s*	*P, Watt*	*Q, m^3/s*	*P, Watt*	*Q, m^3/s*	*P, Watt*
1	1.5	0.303	3355	0.412	4394	0.539	5553	0.682	6826	0.842	8205
2	2	0.35	5285	0.476	6949	0.622	8816	0.787	10880	0.972	13133
3	2.5	0.391	7488	0.532	9868	0.695	12549	0.88	15524	1.087	18783
4	3	0.428	9935	0.583	13112	0.762	16700	0.964	20690	1.19	25072
5	3.5	0.463	12603	0.63	16650	0.823	21230	1.041	26331	1.286	31943
6	4	0.495	15475	0.673	20461	0.88	26110	1.113	32410	1.374	39350
7	4.5	0.525	18539	0.714	24527	0.933	31318	1.181	38898	1.458	47257
8	5	0.553	21782	0.753	28832	0.983	36833	1.245	45771	1.537	55634
9	5.5	0.58	25196	0.79	33364	1.031	42639	1.305	53008	1.612	64456
10	6	0.606	28773	0.825	38112	1.077	48723	1.363	60592	1.683	73703

Table 2. Dependence of the size of the hydro turbine on its power when the water consumption is constant

№	*H, m*	*Q_1=0,2 m^3/s*		*Q_1=0,4 m^3/s*		*Q_1=0,6 m^3/s*		*Q_1=0,8 m^3/s*		*Q_1=1 m^3/s*	
		d_1, m	*P, Watt*	*d_1, m*	*P, Watt*	*d_1, m*	*P, Watt*	*d_1, m*	*P, Watt*	*d_1, m*	*P, Watt*
1	1,5	0,244	2338	0,345	4278	0,422	6104	0,487	7850	0,545	9533
2	2	0,227	3383	0,321	6226	0,393	8932	0,454	11546	0,507	14088
3	2,5	0,215	4336	0,303	7996	0,372	11502	0,429	14909	0,48	18238
4	3	0,205	5301	0,29	9781	0,355	14088	0,41	18287	0,458	22403
5	3,5	0,197	6277	0,279	11579	0,342	16688	0,394	21679	0,441	26583
6	4	0,191	7262	0,27	13389	0,33	19302	0,381	25087	0,427	30777
7	4,5	0,185	8256	0,262	15211	0,321	21929	0,37	28508	0,414	34986
8	5	0,18	9259	0,255	17044	0,312	24569	0,361	31942	0,403	39209
9	5,5	0,176	10270	0,249	18886	0,305	27220	0,352	35390	0,394	43445
10	6	0,172	11288	0,244	20739	0,299	29882	0,345	38849	0,385	47694

Let's compare Tables 1 and 2. In Table 1, the water consumption in a 2.5 m water column is 7488W, and the power released by the hydro turbine is 391l/s. In table 2, the water consumption in a 2.5 m water column is 7996W in the hydro turbine at water consumption Q=400l/s. Based on the comparison of the results obtained in the tables, when the dimensions of the hydro turbine are changed depending on the water consumption, the power released in the hydro turbine will be higher than if we kept the dimensions of the hydro turbine unchanged.

4.2 Results obtained on the basis of mathematical modeling

The graphs in Figure 4 and 5 show the relationship between water consumption and hydroturbine efficiency versus water head for the case of constant turbine supply cylinder size.

From the graphs in Figures 4-5, it can be seen that the efficiency of the hydroturbine when the hydroturbine size is changed depending on the water consumption is higher than if we keep the hydroturbine size constant.

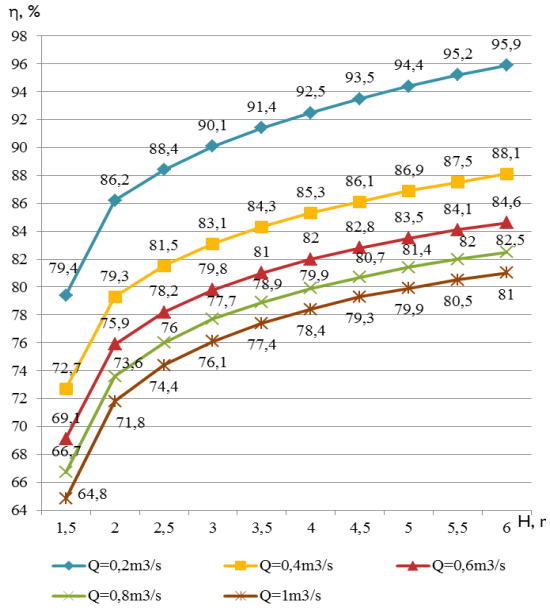

Fig. 4. Variation of hydro turbine efficiency depending on water level when water consumption is constant

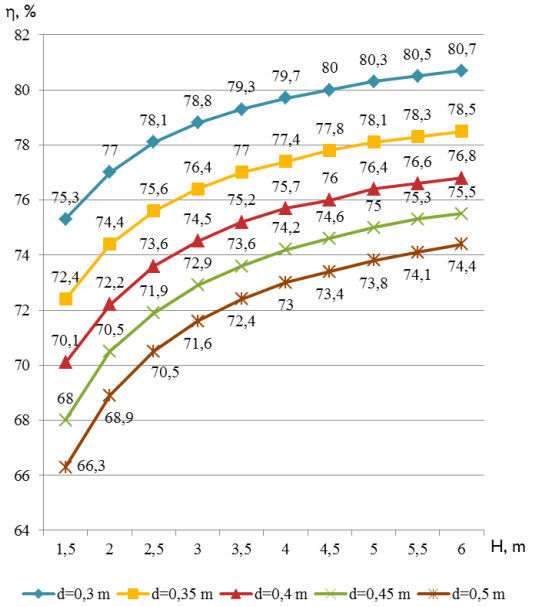

Fig. 5. Variation of hydroturbine efficiency as a function of water level when the size of the hydroturbine supply cylinder remains constant

From the graphs in Figures 4 and 5, it can be seen that the efficiency of the hydroturbine when the hydroturbine size is changed depending on the water consumption is higher than if we keep the hydroturbine size constant [11,12].
Based on the results obtained above, in the Comsol multiphysics software system below, the dependence of the velocity of water at the exit of the impeller nozzle on the K-ε interface on the water column, the energy dissipation in the case of the water column dependence, the dependence of the radius of the hydroturbine supply pipe on the water column at a constant water consumption of Q=200l/s, at a water column of 2 m depending on the water consumption, the radius of the hydro turbine supply pipe depends on the water consumption, the graph of the dependence of the speed of water at the exit of the impeller nozzle on the angle of location of the blade in relation to the radial direction is shown.

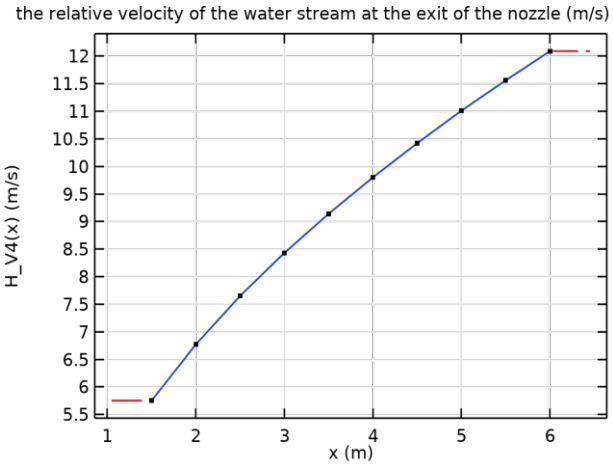

Fig. 6. Dependence of the velocity of water at the outlet of the impeller nozzle on the water column

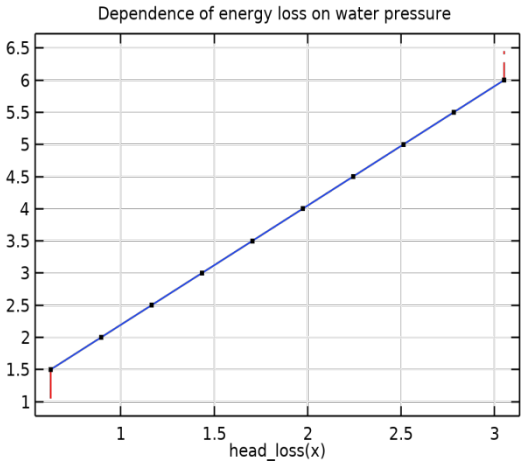

Fig. 7. Energy loss due to water column

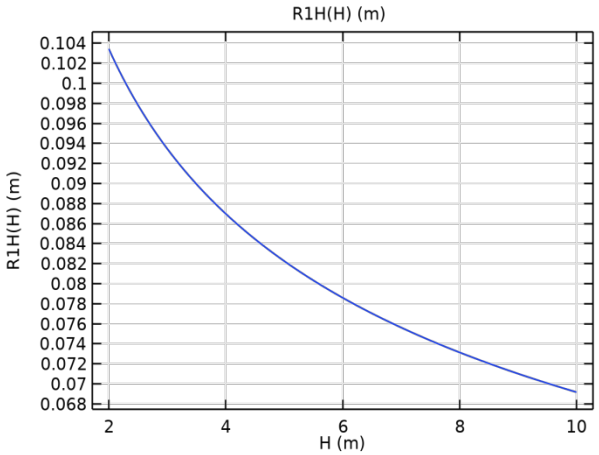

Figıo 8. Dependence of the radius of the hydro turbine supply pipe on the water column at a water consumption of Q=200l/s

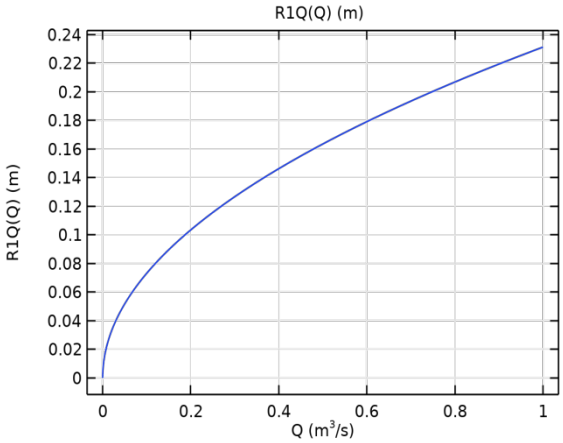

Fig. 9. Dependence of the radius of the hydroturbine supply pipe on the water consumption according to the water consumption in the 2 m water column

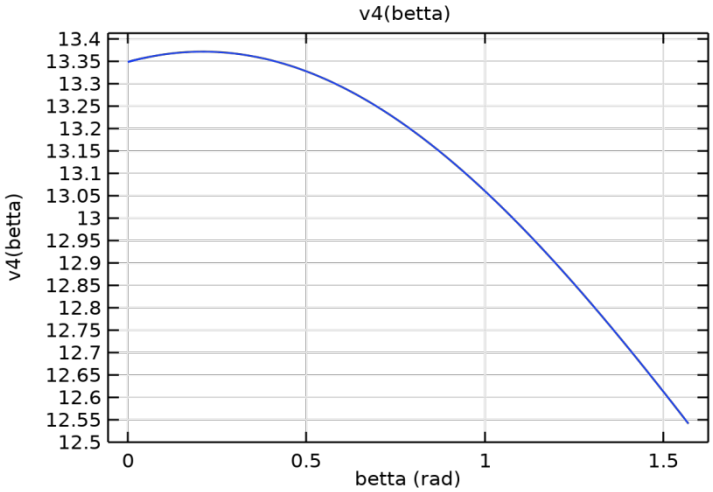

Fig. 10. Dependence of the location angle of the vane directing the speed of water at the exit from the nozzle of the impeller relative to the radial direction

By using the graphs in the above figures, the dimensions of the hydroturbine, the optimal values of the speed of water exit from the impeller, and the energy parameters that occur in the impeller of the hydroturbine are used to increase the efficiency of the hydroturbine [13,14].

5. Conclusion

In the case of investigation, the following results were obtained:

- the hydroturbine made by changing its size according to the water consumption, under the same conditions as the hydroturbine made without changing its size, in a water column of 2.5 m, when the water consumption is Q=400l/s, the power released by the wheels of the hydroturbine was determined. As a result, it was determined that the power released by the hydro turbine impeller made by changing the dimensions according to the water consumption is 4.3% higher than the power released by the hydro turbine impeller made without changing the size.
- The diameter of the active working wheel is slightly different from the diameter of the reactive working wheel. Therefore, the speed of this active wheel will be close to the speed obtained in the experiment for the reactive working wheel.
- The diameter of the active impeller differs little from the diameter of the reactive impeller. Therefore, the speed of this active wheel will be close to the speed obtained in the experiment for the reactive impeller.

- The active wheel can be placed outdoors, the complex is convenient to assemble, perform various services, and its advantage is that the operation mode can be monitored visually.
- One input stream to the hydraulic unit is used twice. Accordingly, the energy of water is fully utilized. Works effectively at high speed even at low pressure.

The outer and inner shafts are connected in a simple way, and work effectively in low pressure water sources. The design of the hydraulic unit is simple, it is easy to operate and implement. The lower active impeller is devoid of the disadvantages mentioned above, i.e. does not show upward pressure. There is no vortex movement in the water flow that enters the second impeller, which manifests itself in the absence of energy losses, since two different types of impellers (reactive and active) are used.

References

1. A. Mirzaalimov, J. Gulomov, R. Aliev, N. Mirzaalimov, S. Aliev, A study of silicon p-structures with mono and multifacial photosensitive surfaces, *Information technologies mechanics and optics* **22**, 25-32 (2022)
2. J.J. Gulomov, R. Aliev, N.A. Mirzaalimov, B.D. Rashidov, J. Aliyeva, Study of Mono- and Polycrystalline Silicon Solar Cells with Various Shapes for Photovoltaic Devices in 3D Format: Experiment and Simulation, *Journal of Nano- and Electronic Physics* **14**, 0501 (2022)
3. R. Aliev, L. Usmanov, M. Komilov, S. Aliev, O. Mirkomilov, N. Mashrabjonova, Hybrid solar photo and wind electric module UzR, Patent No. FAP 02170 (Application No. FAP20220196)
4. R Aliev, O.O. Bozarov, O.O. Mirkomilov, S.R. Aliev, N. Abbasova, Hybrid solar photo and hydroelectric energy device UzR, Patent No. FAP 02169 (Application No. FAP20220197)
5. Sh.B. Umarov, Kh.B. Sapaev, Sh.M. Atajiev, U.A. Bokizhonov, Kh.A. Muminov, Variable Frequency Automated Solar Panel Cooling System, *Universum: Engineering Sciences* **6**, 75 (2020)
6. F.G. Al-Amri, T. Maatallah, R. Zachariah, A.T. Okasha, A.K. Alghamdi, Enhanced Net Channel Based-Heat Sink Designs for Cooling of High Concentration Photovoltaic (HCPV) Systems in Dammam City, *Sustainability* **14**, 4142 (2022)
7. N.E. Kochin, I.A. Kibel, N.V. Roze, Theoretical hydromechanics, State publishing house of physical and mathematical literature, Moscow (1963)
8. D. Adanta, M. Kurnianto, Effect of the number of blades on undershot waterwheel performance for straight blades, *IOP Conf. Series: Earth and Environmental Science* **431**, 012024 (2020)
9. S.F. Ergashev, R.U. Aliyev, O.O. Bozarov, H.S. Osarov, Efficiency of a nozzle jet hydroturbine with internal direction device, *Technical science and innovation* **4**, 175-182 (2022)
10. O.O. Bozarov, H.S. Osarov. Energy parameters of a nozzle hydroturbine with a guide device. *Scientific and Technical Journal of NamIET* **4**, 295-301 (2022)
11. G. Kushakov, D. Kodirov, Study on the combined use of solar and water energy in power supply systems, *E3S Web of Conferences* **377**, 01001 (2023)
12. A. Ahmedov, O. Tursunov, R. Khakimov, M. Rakhmataliev, D. Kodirov, Economic efficiency in the use of solar energy: A case study of Agriculture in Uzbekistan, *IOP Conference Series: Earth and Environmental Science* **614**(1), 012031 (2020)
13. O. Bozarov, D. Kodirov, O. Tursunov, S. Khushiev, G. Tashkhodjaeva, S. Mirzaev, Mathematical description of water flow quantity for microhydroelectric station, *IOP Conference Series: Earth and Environmental Science* **614**(1), 012032 (2020)
14. K. Muratov, O. Tursunov, D. Kodirov, E.I. Ugwu, A. Durmanov, The use of renewable energy sources in integrated energy supply systems for agriculture, *IOP Conference Series: Earth and Environmental Science* **614**(1), 012007(2020)